



Regional modulation of the ankle plantarflexor muscles associated with standing external perturbations across different directions

J. W. Cohen¹ · A. Gallina² · T. D. Ivanova¹ · T. Vieira^{3,4} · D. J. McAndrew⁵ · S. J. Garland¹

Received: 25 May 2019 / Accepted: 15 November 2019 / Published online: 23 November 2019
© Springer-Verlag GmbH Germany, part of Springer Nature 2019

Abstract

Maintenance of upright standing posture has often been explained using the inverted pendulum model. This model considers the ankle plantarflexors to act as a single synergistic group. There are differences in muscle properties among the medial and lateral gastrocnemius (MG and LG, respectively) and the soleus that may affect their activation. Twelve volunteers participated in an investigation to determine whether the activation of the ankle plantarflexor muscles was modulated according to perturbation direction during unilateral standing perturbations of 1% body mass. High-density surface electromyography (HDS-EMG) was used to determine the amplitude and barycenter of the muscle activation and kinematic analysis was used to evaluate ankle, knee, and hip joint movement. The HDS-EMG amplitude and barycenter of MG and LG were modulated with the perturbation direction (MG $p < 0.05$; LG $p < 0.01$; one-way repeated-measures ANOVA). In soleus, the HDS-EMG barycenter modulated across the perturbation direction ($p < 0.01$ for X&Y coordinates), but the HDS-EMG amplitude did not change. A repeated-measures correlation was used to interpret the HDS-EMG pattern in the context of the kinematics. The relative contribution of MG activation compared to the total gastrocnemii activation was significantly associated with ankle dorsi/plantarflexion ($r_{\text{rm}} = 0.620$), knee flexion/extension and abduction/adduction ($r_{\text{rm}} = 0.622$ and $r_{\text{rm}} = 0.547$, respectively), and hip flexion/extension and abduction/adduction ($r_{\text{rm}} = 0.653$ and $r_{\text{rm}} = 0.432$, respectively). The findings suggest that the central nervous system activates motor units within different regions of MG, LG and SOL in response to standing perturbations in different directions.

Keywords High-density surface electromyography · Standing posture · Plantarflexors · Regional modulation

Introduction

Maintenance of upright standing posture is fundamental to human mobility and requires muscular control of the body's centre of mass (CoM) over the base of support. Force production, necessary for stance and movement, is achieved by activating populations of motor units in different muscles. The ankle plantarflexor muscles, comprising soleus (SOL) and medial and lateral gastrocnemius (MG and LG, respectively), are essential for standing balance.

There are three types of motor control strategies commonly described for maintaining standing balance: the ankle strategy, the hip strategy, and taking a step (Winter 1995; Gage et al. 2004). The ankle strategy involves the activation of distal muscles first, in particular the ankle plantarflexors to control the position of the body (approximated to an inverted pendulum) during small, backward surface translations (Horak et al. 1990). With larger perturbations or when standing over narrow surfaces, a hip strategy would

Communicated by Winston D Byblow.

✉ S. J. Garland
jgarland@uwo.ca

¹ Faculty of Health Sciences, University of Western Ontario, London, ON, Canada

² Graduate Program in Rehabilitation Science, University of British Columbia, Vancouver, BC, Canada

³ Laboratorio di Ingegneria del Sistema Neuromuscolare (LISiN), Dipartimento di Elettronica e Telecomunicazioni, Politecnico di Torino, Turin, TO, Italy

⁴ PoliToBIOMed Lab, Politecnico di Torino, Turin, TO, Italy

⁵ Faculty of Science, Medicine and Health, University of Wollongong, Wollongong, NSW, Australia

be preferentially incorporated to firstly recruit the hip musculature to keep the CoM over the base of support (Horak and Nashner 1986). When a perturbation occurs that is too large for individuals to maintain body position with either the ankle or hip strategy, they will take a step, effectively changing their base of support to regain balance (Horak and Nashner 1986; Maki and McIlroy 1997).

The classic biomechanical model for controlling the CoM in quiet standing, the inverted pendulum model, has been derived from joint angle analyses and predicts that the CoM and centre of pressure (CoP) position are phase locked (Winter 1995). The inverted pendulum model considers the plantarflexors to function as the main synergistic group; accordingly, it does not consider the different properties of the ankle plantarflexor muscles. Gastrocnemius, with its larger proportion of fast-twitch motor units, produces larger forces and faster rates of force development than SOL (Garnett et al. 1979). When healthy subjects stand at ease, gastrocnemius motor units are activated intermittently, with recruitment occurring during specific body positions (i.e., during fast and forward sways) (Vieira et al. 2012). Soleus, on the other hand, has a larger proportion of slow-twitch motor units that slowly modulate their firing rate over several seconds with anterior–posterior sway (Mochizuki et al. 2005). In addition to these properties, previous research has shown that the MG and SOL are activated independently above tonic frequencies of 0–0.2 Hz (Loram et al. 2005). However, in response to external stretch or during an active contraction of either muscle, the two muscles effectively act as a single synergist at frequencies above 1 Hz (Loram et al. 2005).

Our knowledge of how the central nervous system modulates the activation of different ankle plantarflexor muscles to control the CoM position during standing balance perturbations remains incomplete. A study conducted by Staudenmann et al. (2009) has revealed an association between regional variation in triceps surae activity and the production of ankle torque during isometric contractions in different planes. Such variation in muscle activity may be critical for standing control. Henry et al. (1998) also described that the MG and SOL respond in a directionally specific manner to external perturbations produced through support surface translation with maximal activation occurring in response to diagonal translations. Research using high-density surface electromyography (HDS-EMG) has uncovered a spatial localization of activation within MG and LG in response to specific directional sway during quiet standing (Vieira et al. 2009). Spatial variations in the activation of triceps surae have been substantiated using magnetic resonance imaging (MRI) (Segal and Song 2005; Kinugasa et al. 2011). Kinugasa et al. (2011) concluded that an increase in contraction intensity from 20 to 60% of maximal voluntary contraction does not necessarily result from a whole muscle contraction, but rather the activation of specific regions. Taken together,

these findings support the notion that, rather than activation of a single plantarflexor volume, there may be preferential modulation of the ankle plantarflexor muscles in response to standing balance perturbation.

Previous studies have used voluntary ramp contractions, and quiet standing trials to determine regional activity within the plantar flexor muscles. The purpose of this study was to examine if the MG, LG, and SOL muscles are modulated regionally during a functional task of unilateral standing perturbations across different perturbation directions. Measurements of joint kinematics and CoP excursions enabled the muscle modulation to be put into the context of a balance strategy during unilateral stance. It was hypothesized that regional modulation of the MG, LG and SOL would be associated with the direction of the perturbations and the kinematic response to the perturbations.

Materials and methods

Ethical approval

This study involved 12 healthy participants (Table 1). Participants were included if they could stand on one leg for 1 min without excessive postural sway (determined by average CoP velocity and 95% ellipse area). Participants were excluded if they had any previous injury to their dominant leg within the past 6 months, or any health conditions that negatively impacted balance (e.g. musculoskeletal disorders). Each participant provided written consent, the study conformed to the latest revision of the Declaration of Helsinki and was approved by the Health Sciences Research Ethics Board at Western University and the Clinical Research Ethics Board of the University of British Columbia.

Experimental protocol

Participants stood balanced on one leg (unilateral stance) on a force platform (OR6-6, Advanced Mechanical Technology, Watertown, MA, USA) with a standardized foot position. Participants were instructed to bend their non-weight-bearing limb and position it next to the support limb

Table 1 Participant characteristics

Age (years)	34 ± 12
Sex	
Male	6
Female	6
Height (cm)	176.0 ± 9.8
Mass (kg)	68.7 ± 12.8
BMI	22.2 ± 2.3

Values are mean ± SD

but not touching (see Fig. 1a). External loads were applied via a cable-pulley system attached to a belt secured around the pelvis of each participant (Fig. 1a). Participants were instructed to stand on one leg in one of five perturbation direction conditions. At 0° (Front), the foot was directly forward and the perturbation caused an anterior translation of the body. In the other four conditions, the pulley system was maintained in the same position but participants stood with their foot pointing 30° or 60° to the participant’s left to obtain a perturbation directed toward the right (30R and 60R, respectively), or pointing 30° or 60° to the participant’s right to obtain a perturbation toward the left (30L and 60L, respectively). The notation of the ‘L’ or ‘R’ corresponds to the direction of the perturbation, not the foot placement. The unilateral stance was used to prevent the postural response being executed through bilateral compensation, ensuring all postural responses were elicited by the muscles of the standing leg only (Dos Anjos et al. 2018). Participants selected their preferred leg for unilateral stance; all participants chose the right leg. Previous research has indicated that unilateral balance is not different between the functionally dominant and non-dominant leg in healthy individuals (Hoffman et al. 1998; Lin et al. 2009).

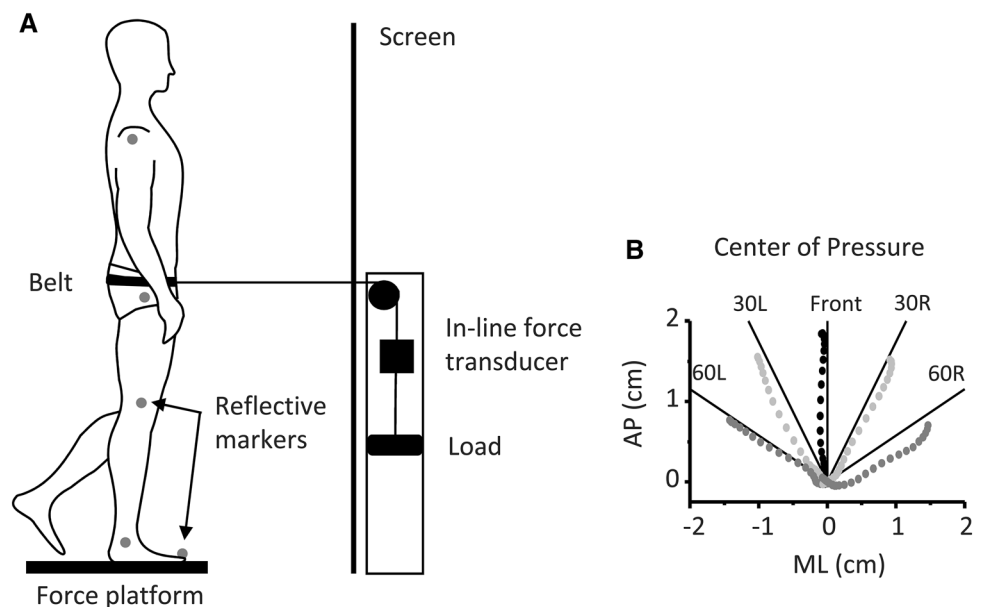
The order of the five directions for the external perturbations was randomized within and across participants. Five perturbation trials in each of the five directions were induced by dropping a load of one percent of body mass from a 40 cm distance into a basket attached with a cable to the belt placed around the participants’ pelvis. A load of 1% body mass was chosen, because pilot testing revealed that a perturbation above 1% often elicited a step or a large response of the hips and trunk, showing that the perturbation exceeded the capacity of the ankle plantarflexors to maintain

upright stance. The load remained in the basket for 10 s and then the trial ended. Participants were blinded to the timing of the load drops by a screen obstructing their view (Fig. 1a). They were instructed to avoid taking a step and return to the starting position after the perturbation. The load application was detected by a force transducer (MLP-150, Transducer Techniques, Temecula, CA, USA) in-line with the cable and basket (Fig. 1a).

High-density surface EMG recordings

Placement of the HDS-EMG grids was performed with participants lying prone with the ankle in 90° plantar flexion and was guided by the participants’ anatomical structures. The distal edges of the superficial aponeurosis of MG and LG, the fascial space between the two muscles, and the medial and lateral edges of gastrocnemius and SOL were identified using an ultrasound imaging system (LogicScan 64 LT-1T; Teleded, Vilnius, Lithuania) and were marked on the skin. Four 16-channel semi-disposable arrays with an interelectrode distance of 10 mm (OTBIOELECTRONICA, Torino, Italy) were placed over MG and LG. To avoid EMG detection from the distal region of gastrocnemius where EMGs have different characteristics as propagating action potentials can be observed (Gallina et al. 2013), the first array was placed 20 mm above the insertion of the MG on the Achilles tendon and the three additional arrays were placed superior to the first. This formed a grid of 16×4 electrodes with 10 mm and 25 mm centre-to-centre distance in the medio-lateral and proximo-distal directions, respectively. The grid was aligned to the fascial space between MG and LG in such a way that nine columns of electrodes were on the MG, and seven columns were on the LG. Thus,

Fig. 1 a Experimental set up. Schematic of experimental set up for applying perturbations that result in a pull in anterior direction (Front). Markers denote segments used to calculate ankle, knee, and hip joint angles. **b** Grand average of the CoP position across all 12 participants from 0 to 250 ms after the perturbation onset. R (right) and L (left) stand for the direction of perturbation pull; the numbers (30 and 60) show the perturbation direction in degrees from directly anterior (Front)



the grid over MG consisted of nine columns and four rows (80×75 mm area), and over LG, it was seven columns and four rows (60×75 mm area). A HDS-EMG grid (semi-disposable matrix, OTBioelettronica, Torino, Italy) placed on SOL consisted of 64 electrodes arranged in 13 columns and 5 rows (with an electrode missing in 1 of the rows), spaced 8 mm apart with a total area covered of 96×40 mm. The matrix was centered on the Achilles tendon and was placed 10 mm below the distal insertion of MG. The arrays and grid were held in place using bio-adhesive foam, and conductive paste ensured optimal contact between the skin and the electrodes (see schematic of the HDS-EMG sensor placement in Fig. 2a). A grounding strip was placed around the ankle. EMG signals were collected in monopolar modality; thus, two reference electrodes (2×3.4 cm; conductive hydrogel; Kendall Covidien, Mansfield, MA, USA) were placed on the patella (for MG and LG) and the medial malleolus (for SOL) and connected to the monopolar connectors. Signals were amplified 500 times using HDS-EMG amplifier (128-channel EMG-USB with OTBioLab software v.2.0.5; OTBioelettronica, Torino, Italy) and digitized at 2048 Hz using a 12-bit analog-to-digital converter.

Kinematic and kinetic data

Twenty-two passive reflective markers were affixed to participants according to a modified Helen Hayes marker set

(Kadaba et al. 1989) to allow for motion capture of the upper and lower limbs and the trunk. Ten high-speed digital cameras (Motion Analysis Corp, Santa Rosa, CA, USA) sampled the movement of the reflective markers at 100 Hz. Two static double-leg standing trials were recorded to determine marker orientations and positions of the joint centers of rotation. Medial femoral condyle and malleolus markers on both legs were removed prior to the unilateral stance trials. Kinetic data were collected using a single floor-mounted force platform (detailed above) sampled at 100 Hz. Kinetic and kinematic data were collected by the Motion Analysis system with Cortex v.7.2 software. The force signal from the in-line load cell (see above), recorded on both Motion Analysis and EMG systems, was used for establishing the onset of the perturbations and to synchronize the recording systems.

Data analysis

The onset of each perturbation was determined by threshold crossing on the filtered force signal (low-pass, Butterworth second order; 8 Hz cut-off) (Fig. 3). The threshold was calculated as mean + 2 SD for a 500 ms epoch prior to the perturbation onset.

All EMG analyses were performed using MATLAB R2013b (The MathWorks, Inc., Natick, MA, USA). EMG

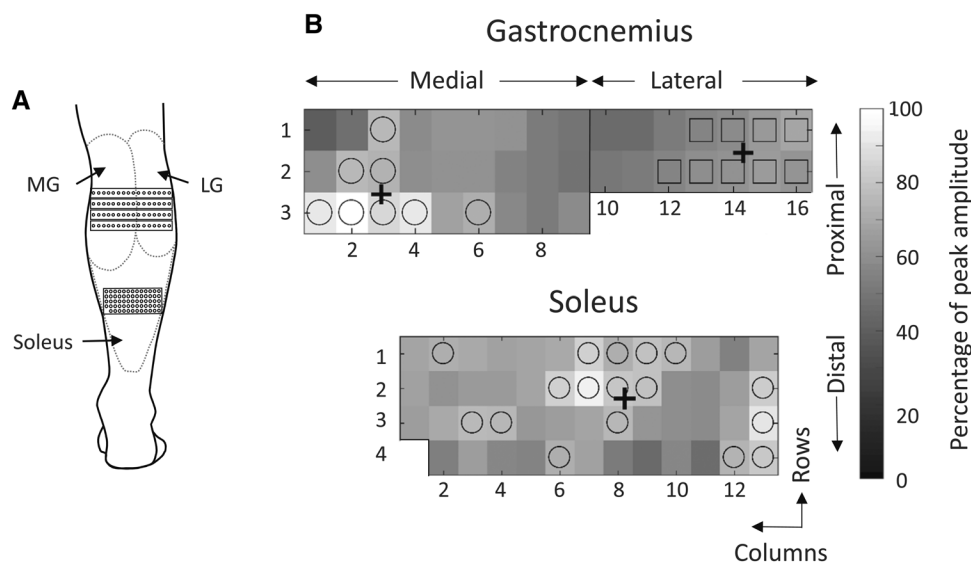
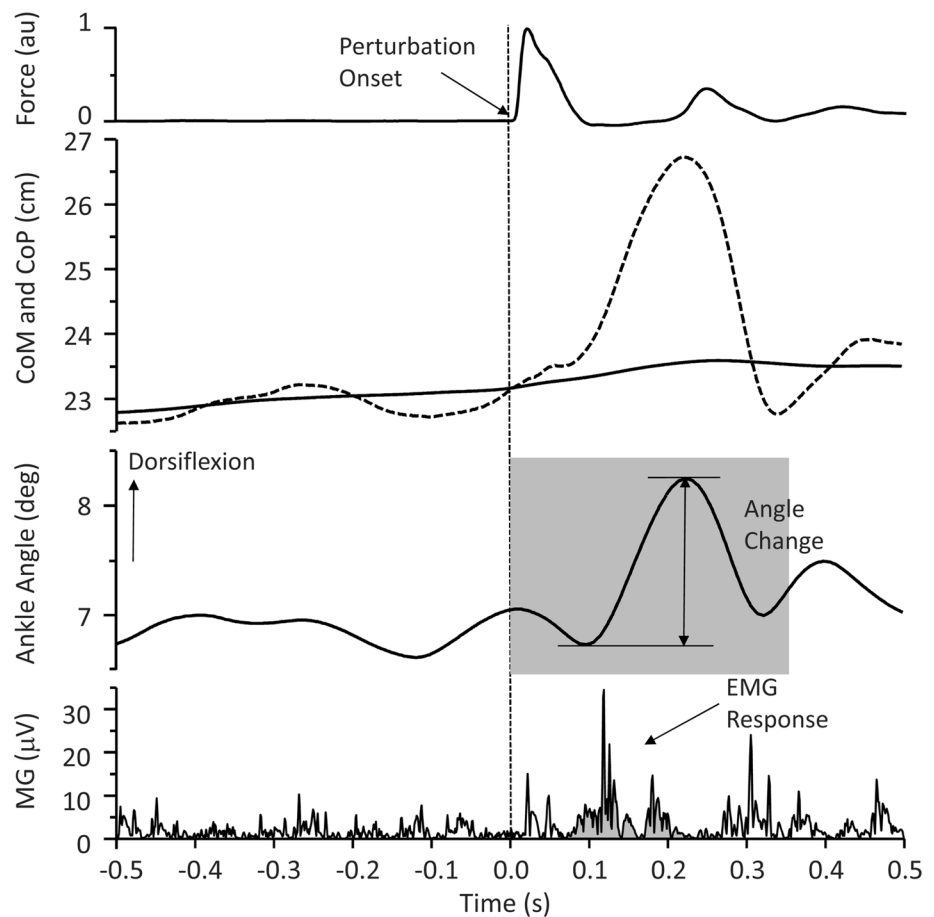


Fig. 2 High-Density surface EMG. **a** Placement of the High-Density surface EMG sensors over the plantar flexors. Four 16 electrode arrays were placed over the gastrocnemius, with 9 electrodes on the medial gastrocnemius (MG), and 7 electrodes on the lateral gastrocnemius (LG). The most distal array is placed 20 mm above the MG superficial aponeurosis. A grid of 64 electrodes (13 columns and 5 rows) was placed over the soleus. **b** EMG activity maps of a single participant for a perturbation directly anterior (“Front”). The top maps are

for medial (left) and lateral (right) gastrocnemius and the bottom map is for soleus muscle. The lighter (white) filled squares indicate higher EMG amplitude (more activation), whereas the darker (black) filled squares indicate lower EMG amplitude (less activation). The channels with amplitude exceeding the 70% of the highest activity for each muscle are indicated with squares for the lateral gastrocnemius and circles for medial gastrocnemius and soleus. These channels were used to calculate the barycenters indicated with black crosses

Fig. 3 Kinetic, kinematic and EMG measures. Single-channel medial gastrocnemius (MG) EMG (bottom row), ankle dorsiflexion/plantarflexion angle (third row), CoP (dotted line, second row) and CoM (solid line, second row) and force trace (top row) registering the release of load for a single perturbation at 0° (Front). The onset of perturbation is denoted with vertical dashed line. The shaded rectangle indicates the time window where the kinematic parameters were measured from the minimum located close to the perturbation onset to the peak (in this case, ankle dorsiflexion/plantarflexion angle change). The plantarflexors EMG bursts (only MG is presented) window from 70 to 280 ms (gray shade) coincides with the initiation of the kinematic response to the perturbations



signals were band-pass filtered (Butterworth filter, fourth order, 20–400 Hz). EMG channels showing artifacts due to poor contact of EMG sensors with the skin, as determined by visual inspection (1–2 channels per grid; less than 10% of the channels), were replaced by the linear interpolation of up to four adjacent channels. EMG signals were analyzed in single differential configuration calculated along the rows of the grids, resulting in 13×4 and 9×3 EMG signals from SOL and MG muscles, respectively. As the superficial aponeurosis ends more proximally in LG than MG, in some participants, the seven electrodes of the most distal row were lying over LG region where propagating potentials are observed (see above). These electrodes were excluded from the analysis for all participants, providing 7×2 signals for the LG muscles. For each participant, the timing of the five perturbation trials for each perturbation direction was determined from the in-line force signal. Epochs from 500 ms before to 280 ms after each perturbation were extracted from the EMGs and used to estimate the amplitude of the response for each channel of the grid. To improve the detection of the response to perturbation, EMGs collected from each channel of the grid were full wave rectified and averaged across the five perturbations. Averaging of EMGs collected from triggered motor tasks has been shown to be a valid method

to detect the timing of muscle activation in conditions of low signal-to-noise ratio (Hug et al. 2006).

Two epochs were selected for analysis. Baseline EMG activity was determined for the time epoch 500 ms prior to the perturbation onset; muscle activation in response to the perturbation was calculated between 70 and 280 ms following the perturbation, where the highest EMG response was found (Fig. 3). The amplitude distribution of the MG, LG and SOL recordings during every perturbation direction was obtained by computing the average rectified value (ARV) for each channel during the selected epochs. The proportion of MG activation in relation to the total gastrocnemius activation was calculated as

$$MG \% = \frac{\sum ARV_{ch}^{MG}}{\sum ARV_{ch}^{MG} + \sum ARV_{ch}^{LG}} \cdot 100\%$$

and is hereafter referred to as MG %. The corresponding LG % is computed as: 100—MG %.

To improve the accuracy of distribution measures, muscle activity in MG, LG and SOL was quantified from the cluster of channels with amplitude above 70% ARV of the channel with highest activity for each muscle (Vieira et al. 2010). The amplitude of EMG activity of each muscle was

calculated by averaging the ARVs of these channels. To identify any variations in the amplitude distribution between perturbation directions, the barycenter of the cluster channels was computed as

$$\text{barycentre} = \frac{\sum \text{ARV}_{\text{ch}} \text{POS}_{\text{ch}}}{\sum \text{ARV}_{\text{ch}}}$$

with ‘ch’ being each channel in the cluster, ‘ARV’ being their average rectified value (measure of amplitude) and ‘POS’ being their position along either rows or columns in the grid (Gallina et al. 2013). The barycenter is the centroid of the identified active muscle region and provides an estimate for identification of regional modulation within muscles. EMG amplitude distribution maps of MG, LG and SOL muscles from an individual participant’s Front perturbation are presented in Fig. 2b. For each participant, the overall activation of MG, LG and SOL muscles during different perturbation directions was assessed by computing the mean amplitude of all the channels of the respective grids (i.e. not only those exceeding the 70% threshold level noted above).

Kinematic data were analyzed using Orthotrac v.6.6 (Motion Analysis Corp, Santa Rosa, CA, USA). Body segment angles were calculated in the sagittal and frontal planes for the ankle, knee, and hip of the stance leg for ankle dorsiflexion/plantarflexion, knee flexion/extension, knee abduction/adduction, hip abduction/adduction, and hip flexion/extension. The calculated angles were aligned with the force signal, filtered with a fourth-order low-pass Butterworth filter (cut-off frequency = 6 Hz), and measured using Spike2 v.6.17 (Cambridge Electronic Design Ltd., Milton, Cambridge, UK) during a 280 ms epoch post-perturbation onset. As the perturbations were administered randomly, participants were unaware of the timing of the perturbation. Participant’s EMG burst occurred at a latency of approximately 70 ms. The kinematic angle change of each segment in response to the perturbation was measured by taking the minimum kinematic angle at 70 ms after the onset of the perturbation, and the maximum peak within the next 280 ms (70–350 ms) (Fig. 3).

The position of the CoM in the medio-lateral and anterior–posterior directions was calculated as

$$\text{CoM}_x = \frac{1}{M} \sum_{i=12} m_i x_i \text{ or } \text{CoM}_y = \frac{1}{M} \sum_{i=12} m_i y_i,$$

where m_i is the body segment mass; x is the medio-lateral and y is the anterior–posterior coordinate for the CoM of that segment (x_i or y_i) and M is the whole body mass.

The CoM traces were aligned with the force signal (Fig. 3), filtered with a fourth-order low-pass Butterworth filter (cut-off frequency = 50 Hz) and measured using Spike2 v.6.17 at two time points: 200 ms prior to the perturbation onset and at perturbation onset. To evaluate the direction of

the CoM sway just prior to the perturbation, the displacement of the CoM in anterior–posterior (ΔCoM_y) and medio-lateral (ΔCoM_x) direction between the two time points was calculated and the angle between the vector (formed by the coordinates of the CoM) and the positive anterior–posterior axis was calculated by

$$\text{Direction of CoM} = \tan^{-1} \left(\frac{\text{CoM}_x}{\text{CoM}_y} \right) \frac{180}{\pi}.$$

Distinction was made between positive and negative values in both directions, resulting in a single value in degrees (-180° to 180°) which represented participant’s direction of CoM in one of the four quadrants. Angle values were referenced to the forward direction (forward right; 0° – 90° , backwards right; 90° – 180° , backwards left; -180° to -90° , forward left -90° to 0°).

CoP position in antero-posterior and medio-lateral directions was calculated from the force platform signals over the 10 s trial, filtered with a fourth-order low-pass Butterworth filter (cut-off frequency = 50 Hz). To determine the overall direction of the CoP position during each perturbation direction, CoP epochs of 500 ms starting 200 ms prior to the perturbation were averaged across the 5 perturbations for each perturbation direction and all 12 participants. CoP grand average for each perturbation direction from 0 to 250 ms after the perturbation onset is shown in Fig. 1b.

Statistical analysis

Statistical analyses were conducted using SPSS v.24 (IBM Corp, Armonk, NY) and R v.3.5.1 (R Core Team, 2013). To determine spatial difference on the HDS-EMG, EMG amplitude and medio-lateral (X) and proximo-distal (Y) coordinates of the barycenter for MG, LG and SOL across different perturbation directions were compared using separate one-way repeated-measures analyses of variance (ANOVAs). There were no outliers, as assessed by examination of studentized residuals for values greater than ± 3 standard deviations, and the data were normally distributed for all parameters (Shapiro–Wilk test, $p > 0.05$). The assumption of sphericity assessed by Mauchly’s test of sphericity was met for the X and Y coordinates of the EMG barycenter ($p > 0.05$). For MG and LG amplitude, the assumption of sphericity was not met ($p < 0.05$) and Greenhouse–Geisser (1959) correction was applied. When a significant main effect was found, Bonferonni’s corrections were used for post hoc planned pairwise comparisons (Student’s t tests, paired samples, two tailed, level of significance $p < 0.0125$). The 60L condition for EMG amplitude, and the X and Y coordinates of the barycenter were compared to the rest of the perturbation conditions (30L, Front, 30R, 60R) to determine the spatial changes on the HDS-EMG. The 60L

comparator was chosen as it portrays the largest change in perturbation direction. Similar results were found using the 60R condition as the comparator.

To determine if the direction of sway prior to the perturbation had an influence on barycenter location, the direction of CoM, medio-lateral and proximo-distal (X and Y) coordinates of the barycenter for MG, LG and SOL, and MG % were compared using separate one-way randomized block design ANOVA. The ‘interventions’ were the four quadrants in which participants’ direction of CoM could move in and the randomized blocks were the participants. There were no outliers, as assessed by examination of the studentized residuals for values greater than ± 3 standard deviations, and the data were normally distributed (Shapiro–Wilk test, $p > 0.05$). The assumption of sphericity assessed by Mauchly’s test of sphericity was met for the direction of CoM and MG % ($p > 0.05$).

A repeated-measures correlation was performed using ‘rmcorr R package’ to determine the relationship between kinematic parameters and regional EMG modulation (i.e. MG %). The repeated-measures correlation is a statistical technique for determining the within-subject association for paired measures assessed on two or more occasions for multiple subjects. Simple correlations (like Pearson’s) require independent observations and when applied to non-independent data often produce biased results. In contrast, repeated-measures correlation does not violate the assumption of independence of observations (Bakdash and Marusch 2017). The correlation yields the rmcorr coefficient (r_{rm}), which is much like a Pearson correlation coefficient (r); bounded by -1 to 1 and represents the strength of the linear association between two variables. Significance is determined by the F -ratio. Statistical significance for all analyses was considered at $p \leq 0.05$.

Results

Perturbations in different directions induced a response in the gastrocnemii appropriate for opposing the direction of the perturbation, revealing a task dependence of the EMG modulation between the muscles. The direction of the CoM movement prior to the onset of the perturbation did not have a significant effect on the MG % or the barycenter position across trials in MG, LG or SOL in any of the perturbation directions (p values ranging from 0.42 to 0.91). The EMG amplitude of the MG, LG and SOL did not have any significant differences ($p > 0.05$) between the perturbation directions during the 500 ms epoch prior to the onset of the perturbation (baseline).

However, in response to the perturbation, the EMG amplitude of MG and LG depended on the direction of the perturbation (MG: $F(2.52, 27.768) = 7.59, p = 0.001$, LG:

$F(2.52, 27.735) = 5.316, p = 0.007$; Fig. 4b). Post hoc pairwise comparisons revealed that the EMG amplitude of MG was significantly lower at 60L compared to all other perturbation directions, i.e. 30L ($p = 0.003$), Front ($p = 0.001$), 30R ($p < 0.001$) and 60R ($p = 0.01$). For LG, the EMG amplitude was significantly lower in response to 30R ($p = 0.002$) and 60R ($p = 0.01$) than at 60L. The fact that the amplitude of the MG response was larger for perturbations toward the right, whereas LG responses were largest when the perturbation was directed towards the left, illustrates a shift in muscle activation between MG and LG depending on the direction

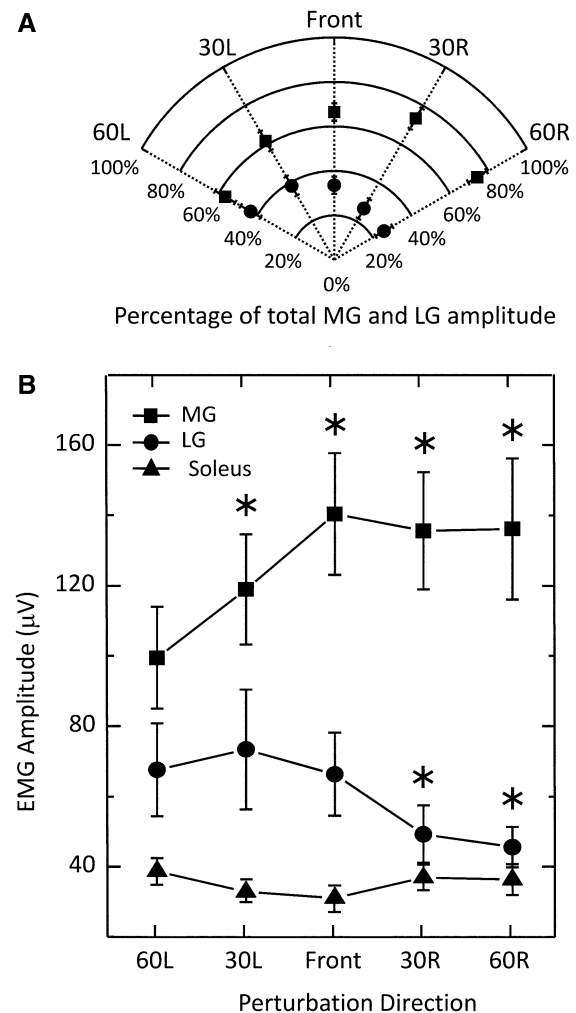


Fig. 4 EMG amplitude for stance leg plantarflexors. **a** Medial (filled square) and lateral (filled circle) gastrocnemii activity are presented as percentage of total gastrocnemii activity during different perturbation directions. There is an approximate 25% increase in MG relative activation from 60L to 60R. **b** EMG amplitude (in μV) for medial (filled square) and lateral (filled circle) gastrocnemius and soleus (filled triangle) muscles at the different perturbation directions. There is an increase in medial gastrocnemius activity from 60L to 60R and a decrease in lateral gastrocnemius activity from 60L to 60R. Data are means \pm standard deviations. *Significantly different values from 60L ($p < 0.0125$)

of the perturbation. The shifts in EMG amplitude for MG, LG and soleus are provided in Fig. 4. There was no difference in SOL EMG amplitude across the perturbation directions (SOL $F(1.675, 18.427, p=0.37$; Fig. 4b).

The perturbation direction had a significant effect on the location of the barycenter within the plantarflexor muscles; the barycenter location shifted medially and proximally as the perturbation direction changed from 60L to 60R (Fig. 5). There was a significant medial–lateral shift across the columns in barycenter location for MG ($F(4,44)=2.596, p=0.04$), LG ($F(4, 44)=8.303, p<0.001$) and SOL ($F(4, 44)=40.125, p<0.001$), while the barycenter proximal–distal shift across the rows was significant only for SOL ($F(2.09, 23.04)=5.00, p=0.01$), but not for MG ($F(1.989, 21.875)=0.774, p=0.47$) or LG ($F(2.684, 29.527)=0.437, p=0.7$). The post hoc pairwise comparison revealed a statistically significant difference from the 60L to 30R condition ($p=0.012$) for the MG barycenter medial–lateral shift across the columns with an average shift of 5.8 mm across the columns (Fig. 5). There were statistically significant differences for the LG barycenter in the medial–lateral shifts across the columns between the 60L to 30R ($p<0.001$) and 60L to 60R ($p<0.001$) with an average shift of 18.0 mm across the columns in both conditions. The SOL post hoc pairwise comparison revealed statistically significant differences in each of the comparisons (60L vs 30L, Front, 30R, 60R, $p<0.001$, average shift of 40 mm) in the medio-lateral plane (across the columns), but only between the 60L–30R ($p=0.01$) and the 60L–60R ($p=0.006$) conditions in the proximo-distal plane (across the rows) with an average shift of 7.3 mm (Fig. 5).

To determine the association between the gastrocnemii EMG regional modulation and the kinematics of the initial postural response (e.g. the first 280 ms), we conducted a repeated-measures correlation analysis with MG % and the kinematic angle changes (Fig. 6). Repeated-measures correlation analysis revealed a significant correlation between the MG % and the kinematic parameters of ankle dorsiflexion/plantarflexion ($r_{rm}=0.620, p<0.001$), knee flexion/extension ($r_{rm}=0.622, p<0.001$), knee abduction/adduction ($r_{rm}=0.547, p<0.001$), hip abduction/adduction ($r_{rm}=0.432, p<0.001$) and hip flexion/extension ($r_{rm}=0.653, p<0.001$). Participants with larger MG % changes (i.e. regional modulation) across the different perturbation directions had stronger correlations, and displayed a pattern of kinematic movements across the different perturbation directions to maintain balance. That is, during the left perturbations (30L and 60L), participants employed an initial pattern of ankle dorsiflexion, knee flexion, knee adduction, hip flexion, and hip abduction to remain balanced and the relative activation of MG was lower (lower MG %; Table 2; Fig. 6). During the right perturbations (30R and 60R), participants initially employed ankle plantarflexion, knee extension, knee abduction, hip extension and hip

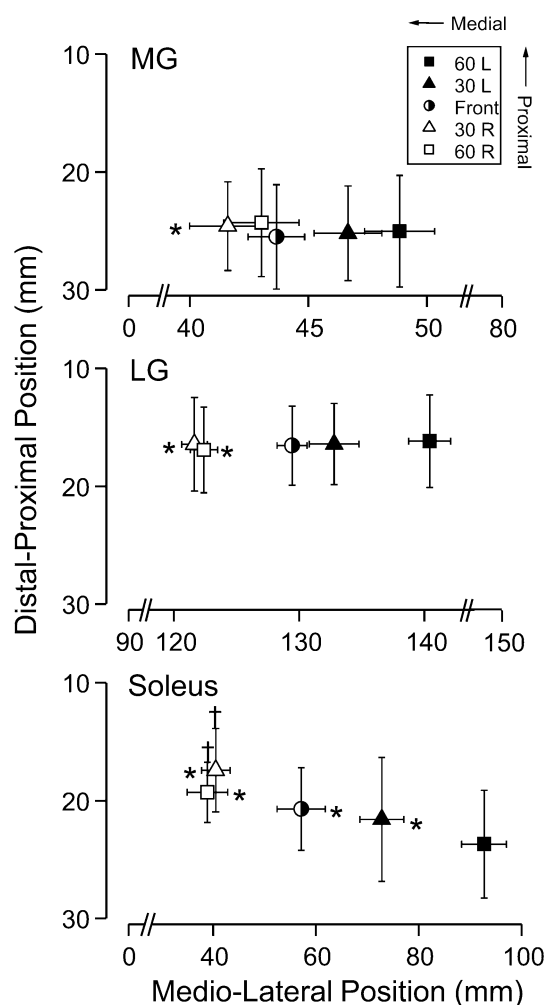


Fig. 5 Barycenters for the five different perturbation conditions in the proximo-distal (across the rows) and medio-lateral directions (across the columns) for the medial and lateral gastrocnemii (MG and LG; top and centre panels) and soleus (bottom panel). For both gastrocnemii (MG and LG), the axes are the distance in mm from the most proximal and medial electrode lying over MG. For soleus, axes are also referenced from the top left (most proximal and medial) electrode of the grid. Data are means \pm standard deviations. *Significantly different values from 60L in the medio-lateral direction ($p<0.0125$). †Significantly different values from 60L in the proximo-distal direction ($p<0.0125$)

adduction to remain balanced with a higher relative activation of MG (higher MG %; Table 2; Fig. 6). Means and standard deviations for kinematic angle changes can be found in Table 2.

Discussion

The regional EMG modulation of the plantarflexor muscles observed in this study suggests that the CNS has the ability to preferentially recruit motor units between the two

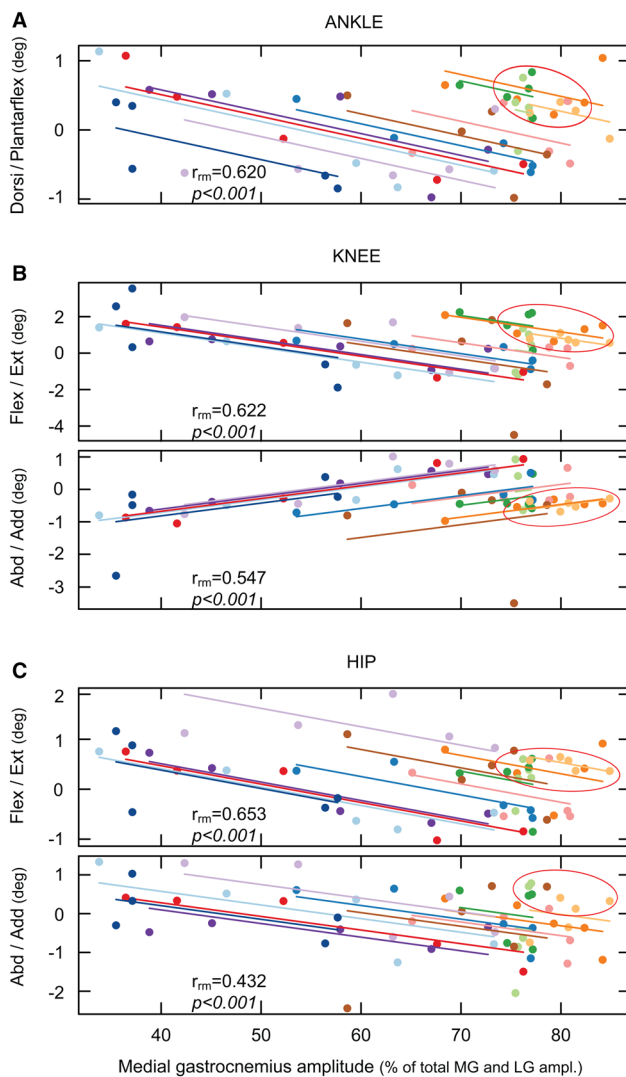


Fig. 6 Repeated-measures correlation between medial gastrocnemius amplitude, presented as percentage of total gastrocnemius EMG activity, and the change of kinematic angle for ankle (top panel), knee (middle two panels) and hip (bottom two panels) during the 280 ms epoch after the onset of perturbations. Each data point for a single participant is an average of the five perturbations per perturbation direction (filled circles) with the lines of best fit, presented in the same color. Positive kinematic angle values indicate dorsiflexion (Dorsiflex), flexion (Flex), and abduction (Abd) and negative values indicate plantarflexion (Plantarflex), extension (Ext) and adduction (Add). Participants who demonstrated less regional EMG modulation tended to cluster (denoted with oval on each graph) and performed only one type of kinematic movement sequence

gastrocnemius heads (MG and LG), and different regions within MG, LG and SOL muscles. This provides evidence that, during unilateral standing perturbations, the ankle plantarflexors are regionally activated in a task-dependent manner. The regional EMG modulation was associated with perturbation direction; that is, the gastrocnemius muscle opposite to the direction of the perturbation showed the

highest modulation relative to the other directions (i.e. perturbations to the right, 30R and 60R, caused higher activity in the MG compared to left perturbations and perturbations to the left, 30L and 60L, caused higher activity in the LG compared to the right perturbations). Perturbation direction also had a significant effect on barycenter location, with positional shifts occurring opposite to the direction of the perturbation in all three muscles (i.e. medially across the columns and proximally across the rows as the perturbation changed from 60L to 60R). Qualitative assessments of participants’ kinematic movements indicated that participants employed different kinematic movement sequences (e.g. dorsiflexion at 60L, plantarflexion at 60R) immediately following the onset of perturbation. This motor pattern correlated significantly with the EMG modulation variations between the gastrocnemii, suggesting a task dependency requirement for the unique muscle modulation.

The regional EMG modulation pattern exhibited during postural control indicates a neural control mechanism in which some of its characteristics have been previously described such as directional-specific activation patterns (Henry et al. 1998), spatial localization of activation in the plantarflexors (Kinugasa et al. 2011), and heterogeneity of muscle activation in relation to force direction (Segal and Song 2005). The unique EMG modulation pattern exhibited in our study integrates these mechanisms to provide a functional model for spatial localization in unilateral balancing tasks. Augmenting the findings of Henry et al. (1998) of maximal activation during diagonal translation, participants in our study exhibited selective maximal activation between the gastrocnemii heads to oppose perturbation direction during diagonal translation. The gastrocnemius activity modulates between the MG and LG to oppose the perturbation direction, effectively activating the motor units situated in a mechanically advantageous position to produce greater torque (see below for detail). Consistent with Kinugasa et al. (2011), we showed that activated regions within a muscle were not distributed randomly, rather our results indicate that the clustering of motor unit activation is exploited during postural control. Segal and Song (2005) demonstrated an increase in plantarflexor activity in the proximal direction after unilateral heel raises. Our findings expand on this with the observed proximal shift in barycenter location within SOL across the different perturbation directions during balancing tasks. Finally, it has been suggested that a muscle is organized into subgroups in which features of the muscle properties can be independently controlled by the CNS (Windhorst et al. 1989). This organization, known as neuromuscular compartments, is believed to be functionally relevant with differences in fiber-type distribution, and/or mechanical advantage (see below) (Chanaud et al. 1991; Butler and Gandevia. 2008). These interpretations agree with our finding of the relative amplitude change between

Table 2 Kinematic angle change

Parameter	Perturbation direction				
	60L	30L	Front	30R	60R
Ankle dorsiflexion (°)	0.41 ± 0.49	0.34 ± 0.39	-0.23 ± 0.84	-0.25 ± 0.98	-0.38 ± 0.98
Knee flexion (°)	0.61 ± 2.40	1.28 ± .90	0.40 ± 1.11	-0.51 ± 1.03	-0.96 ± 2.15
Knee abduction (°)	-0.43 ± 0.99	-0.177 ± 1.06	0.11 ± 0.85	0.14 ± 0.52	0.29 ± 1.55
Hip flexion (°)	0.43 ± 0.66	0.33 ± 0.56	0.13 ± 0.70	-0.14 ± 0.68	-0.16 ± 0.77
Hip abduction (°)	0.03 ± 1.03	0.31 ± 0.58	0.13 ± 0.47	-0.34 ± 0.57	-1.45 ± 1.42

Positive values indicate flexion or abduction, negative values indicate extension or adduction. Values are mean ± SD

the MG and LG (Fig. 4b), which would achieve a greater mechanical advantage for force production.

The recruitment of motor units has previously been shown to be the main mechanism of force modulation in the medial gastrocnemius muscle in response to standing external perturbations (Pollock et al. 2014). As the task itself requires moderate levels of force production, recruitment of motor units may be preferentially utilized. Thus, it seems reasonable that the underlying neural control mechanism for the amplitude and barycenter changes presented here can be attributed to the regionally selective recruitment of motor units.

The regional EMG modulation pattern was related to perturbation direction, with the gastrocnemius muscle opposite to the direction of the perturbation showing the highest EMG modulation, and the barycenters within MG, LG and SOL shifting to oppose the perturbation direction. This EMG modulation pattern has some similarities to the findings of Lee and Piazza (2008) and Vieira et al. (2013) in which the MG and LG showed differences in activation during movements in the sagittal plane. Interestingly, it seems most of the contribution to inversion torque comes from the most medial MG fibers, whereas the contribution of eversion torque comes from the most lateral LG fibers (Vieira et al. 2013). However, to our knowledge, this pattern of regional muscle activation has not been previously observed in a unilateral standing model of balance. It is postulated that this EMG modulation pattern is due to a combination of the anatomical function of the gastrocnemii, the muscle properties related to movement and the nature of the task. The activated motoneurons opposite to the direction of pull would be situated in a mechanically advantageous position. This allows the ankle plantarflexors that insert on a common tendon to be activated in specific regions by the CNS to produce task-specific directional torques. A similar finding was observed in the respiratory muscles such that the Henneman size principle of orderly recruitment is enhanced for directional specificity by a neuromechanical recruitment strategy (Butler and Gandevia, 2008). Heroux et al. (2014) found differential motor unit behavior in SOL and MG during bilateral standing balance. They concluded that

anatomical differences, and possible mechanical advantage, explain the differential behavior of the triceps surae. The EMG modulation patterns found in this study agree with the findings of Butler and Gandevia (2008), and Heroux et al. (2014), because the MG, LG and SOL barycenters shift preferentially towards mechanically advantageous positions. This neural mechanism would ensure that different regions of motor unit pools are preferentially activated to produce a larger proportion of the forces that are required for maintaining unilateral standing balance.

As muscle fibers in the gastrocnemii attach to common Achilles tendon movements about the ankle are often conceived as occurring predominantly as plantarflexion and dorsiflexion. Recently, studies have indicated a contribution of inversion and eversion torques from the gastrocnemii (Vieira et al. 2013) during electrical stimulation to the tibial nerve. Furthermore, in vivo estimates indicate a significant inversion moment arm existing for the human MG muscle, as well as a significant eversion moment arm existing for the LG muscle (Lee and Piazza 2008). It follows that motor units positioned in mechanically advantageous positions are modulated in a medio-lateral direction to produce these inversion and eversion torques. In absolute terms, the gastrocnemii barycenters across directional conditions were more variable in the proximo-distal shifts (across the rows) than in the medio-lateral direction (across the columns) (Fig. 5). Considering that we did not record from the entire gastrocnemius proximo-distal volume, variabilities reported in Fig. 5 may have been underestimated. The high variability of the barycenters' proximo-distal coordinate (across the rows) is in agreement with observations of spatially localized muscle units in MG (Vieira et al. 2015), suggesting there is no preferential recruitment of either proximal or distal units with perturbation direction. Conversely, the small variability of the barycenters in the medio-lateral direction (across the columns) is indicative of a consistent, spatially localized response. Such consistency suggests that gastrocnemius muscle units occupy specific medio-lateral regions, with units located predominantly medially laterally being more likely suited to produce inversion–eversion moments about the ankle, illustrating the functional role of the MG and LG.

It should be noted that the regional modulation pattern occurred as a continuum, with some participants having greater or lesser regional EMG modulation (greater/lesser shifts in barycenter, higher/lower changes in MG %). Participants with less regional EMG modulation (MG % change of < 25%, barycenter shifts of < 2 mm in the medial–lateral plane) can be found clustering within the repeated-measures correlation (Fig. 6), such that they do not employ a similar motor control strategy to those who have a stronger regional modulation. These participants generate one specific kinematic parameter for all the different perturbation directions. They employ an ankle dorsiflexion, knee flexion and adduction, hip flexion and abduction movements regardless of the perturbation direction (Fig. 6). This is markedly different to those participants whose EMG measures are regionally modulated to a higher degree and employ an adaptable pattern of kinematic movements. This qualitative observation demonstrates the functional significance of the regional EMG modulation. Participants that regionally modulate their EMG measures to a lesser degree may rely on co-contraction of other postural muscles, creating stiffer postural responses.

Conclusion

This study supports regional modulation in the ankle plantarflexors (MG, LG and SOL) during unilateral balancing tasks. This EMG modulation pattern was related to perturbation direction, with barycenters shifting medially in MG, LG and SOL, and proximally in SOL, when perturbation direction moved left to right, and the gastrocnemius muscle opposite to the direction of pull of the perturbation showing the highest relative amplitude of activation. This reveals a task-dependent modulation of the ankle plantarflexors during standing external perturbations.

Acknowledgements This work was supported by the Natural Sciences and Engineering Research Council of Canada: NSERC RGPIN 105424-12.

References

- Bakdash JZ, Marusich LR (2017) Repeated measures correlation. *Front Psychol* 8:456. <https://doi.org/10.3389/fpsyg.2017.00456>
- Butler JE, Gandevia SC (2008) The output from human inspiratory motoneurone pools. *J Physiol* 586:1257–1264. <https://doi.org/10.1113/jphysiol.2007.145789>
- Chanaud CM, Pratt CA, Loeb GE (1991) Functionally complex muscles of the cat hindlimb. II. Mechanical and architectural heterogeneity within the biceps femoris. *Exp Brain Res* 85:257–270
- Dos Anjos FV, Gazzoni M, Vieira TM (2018) Does the activity of ankle plantar flexors differ between limbs while healthy, young subjects stand at ease? *J Biomech* 81:140–144. <https://doi.org/10.1016/j.jbiomech.2018.09.018>
- Gage WH, Winter DA, Frank JS, Adkin AL (2004) Kinematic and kinetic validity of the inverted pendulum model in quiet standing. *Gait Posture* 19:124–132. [https://doi.org/10.1016/S0966-6362\(03\)00037-7](https://doi.org/10.1016/S0966-6362(03)00037-7)
- Gallina A, Ritzel CH, Merletti R, Vieira TM (2013) Do surface electromyograms provide physiological estimates of conduction velocity from the medial gastrocnemius muscle? *J Electromyogr Kinesiol* 23:319–325. <https://doi.org/10.1016/j.jelekin.2012.11.007>
- Garnett R, O'donovan M, Stephens J, Taylor A (1979) Motor unit organization of human medial gastrocnemius. *J Physiol* 287:33–43
- Henry SM, Fung J, Horak FB (1998) EMG responses to maintain stance during multidirectional surface translations. *J Neurophysiol* 80:1939–1950
- Heroux ME, Dakin CJ, Luu BL, Inglis JT, Blouin JS (2014) Absence of lateral gastrocnemius activity and differential motor unit behavior in soleus and medial gastrocnemius during standing balance. *J Appl Physiol* 116:140–148. <https://doi.org/10.1152/jappphysiol.0.00906.2013>
- Hoffman M, Schrader J, Applegate T, Kocaja D (1998) Unilateral postural control of the functionally dominant and nondominant extremities of healthy subjects. *J Athl Training* 33:319
- Horak FB, Nashner LM (1986) Central programming of postural movements: adaptation to altered support-surface configurations. *J Neurophysiol* 55:1369–1381
- Horak F, Nashner L, Diener H (1990) Postural strategies associated with somatosensory and vestibular loss. *Exp Brain Res* 82:167–177
- Hug F, Raux M, Prella M, Morelot-Panzini C, Straus C, Similowski T (2006) Optimized analysis of surface electromyograms of the scalenes during quiet breathing in human. *Resp Physiol Neurobi* 150:75–81
- Kadaba M, Ramakrishnan H, Wootten M, Gaine J, Gorton G, Cochran G (1989) Repeatability of kinematic, kinetic, and electromyographic data in normal adult gait. *J Orthop Res* 7:849–860
- Kinugasa R, Kawakami Y, Sinha S, Fukunaga T (2011) Unique spatial distribution of in vivo human muscle activation. *Exp Physiol* 96:938–948
- Lee SS, Piazza SJ (2008) Inversion–eversion moment arms of gastrocnemius and tibialis anterior measured in vivo. *J Biomech* 41:3366–3370
- Lin W-H, Liu Y-F, Hsieh CC-C, Lee AJ (2009) Ankle eversion to inversion strength ratio and static balance control in the dominant and non-dominant limbs of young adults. *J Sci Med Sport* 12:42–49
- Loram ID, Maganaris CN, Lakie M (2005) Human postural sway results from frequent, ballistic bias impulses by soleus and gastrocnemius. *J Physiol* 564:295–311
- Maki BE, McIlroy WE (1997) The role of limb movements in maintaining upright stance: the “change-in-support” strategy. *Phys Ther* 77:488–507
- Mochizuki G, Ivanova TD, Garland S (2005) Synchronization of motor units in human soleus muscle during standing postural tasks. *J Neurophysiol* 94:62–69
- Pollock CL, Ivanova TD, Hunt MA, Garland SJ (2014) Motor unit recruitment and firing rate in medial gastrocnemius muscles during external perturbations in standing in humans. *J Neurophysiol* 112:1678–1684
- Segal RL, Song AW (2005) Nonuniform activity of human calf muscles during an exercise task. *Arch Phys Med Rehab* 86:2013–2017
- Staudenmann D, Kingma I, Daffertshofer A, Stegeman D, Van Dieën J (2009) Heterogeneity of muscle activation in relation to force direction: a multi-channel surface electromyography study on the triceps surae muscle. *J Electromyogr Kinesiol* 19:882–895
- Vieira TM, Windhorst U, Merletti R (2009) Is the stabilization of quiet upright stance in humans driven by synchronized modulations of the activity of medial and lateral gastrocnemius muscles? *J Appl Physiol* 597:1953–1954. <https://doi.org/10.1113/JP271866>

- Vieira TM, Merletti R, Mesin L (2010) Automatic segmentation of surface EMG images: improving the estimation of neuromuscular activity. *J Biomech* 43:2149–2158. <https://doi.org/10.1016/j.jbiomech.2010.03.049>
- Vieira TM, Loram ID, Muceli S, Merletti R, Farina D (2012) Recruitment of motor units in the medial gastrocnemius muscle during human quiet standing: is recruitment intermittent? What triggers recruitment? *J Neurophysiol* 107:666–676. <https://doi.org/10.1152/jn.00659.2011>
- Vieira TM, Minetto MA, Hodson-Tole EF, Botter A (2013) How much does the human medial gastrocnemius muscle contribute to ankle torques outside the sagittal plane? *Hum Mov Sci* 32:753–767. <https://doi.org/10.1016/j.humov.2013.03.003>
- Vieira TM, Botter A, Minetto MA, Hodson-Tole EF (2015) Spatial variation of compound muscle action potentials across human gastrocnemius medialis. *J Neurophysiol* 114:1617–1627. <https://doi.org/10.1152/jn.00221.2015>
- Windhorst U, Hamm TM, Stuart DG (1989) On the function of muscle and reflex partitioning. *Behav Brain Sci* 12:629–644
- Winter DA (1995) Human balance and posture control during standing and walking. *Gait Posture* 3:193–214. [https://doi.org/10.1016/0966-6362\(96\)82849-9](https://doi.org/10.1016/0966-6362(96)82849-9)

Publisher's Note Springer Nature remains neutral with regard to jurisdictional claims in published maps and institutional affiliations.